Adaptive Grid-Voltage Feedforward for Three-Phase Inverters applying Perturb and Observe Algorithm to minimize Current THD

1st Roni Luhtala
Faculty of Engineering and Natural Sciences
Tampere University
Tampere, Finland
roni.luhtala@tuni.fi

2nd Tuomas Messo
Faculty of Information Technology and Communication Sciences
Tampere University
Tampere, Finland
tuomas.messo@tuni.fi

3rd Tomi Roinila
Faculty of Engineering and Natural Sciences
Tampere University
Tampere, Finland
tomi.roinila@tuni.fi

4th Giovanni Spagnuolo
Dept. of Information and Electrical Eng. and Applied Mathematics
University of Salerno
Fisciano, Italy
gspagnuolo@unisa.it

***Abstract*—As the amount of renewable energy increases rapidly, power systems will face novel challenges to maintain power quality. Power quality issues, which usually arise from the grid connection through power-electronic devices, can be reduced by proper control strategies. Grid-connected devices are conventionally optimized into a single operating point, but real performance is affected by the interfaced grid conditions. As the grid conditions change over time, the control performance varies, as does the quality of the power produced. To tackle this issue, the adaptive grid-voltage feedforward is introduced to the control system. The adaptive method, applying a perturb-and-observe algorithm, improves the produced power quality in real time by taking the control system characteristics and the grid conditions into account. The results show the improved power quality in various grid conditions when comparing the adaptive grid-voltage feedforward and the conventional implementations.**

I. Introduction

Electrical energy production is moving, at an accelerated pace, towards climate-friendly distributed generation [1]. Conventional production will be replaced by renewable and distributed generation, which is connected to the grid through fast-switching power electronic converters. Responsibility for the system stability and power quality will move from big synchronous machines to power electronics in renewable-energy dominant grids. During this rapid change, power quality may decrease as the power electronics have been shown to introduce new challenges for power quality and stability issues [2], [3].

Power-electronic devices produce power through semiconductor switches that introduce distortions to the grid that conventional rotating generators did not [4]. The inverters' power quality can be improved by proper control strategies [5]–[7]. An additional control strategy for improving power quality is a proportional feedforward from measured grid voltages [8]. This strategy effectively increases the inverter output impedance and compensates the effect of the grid-voltage harmonics to the output current. [9] This simple implementation is effective at improving power quality when an inverter is operating under distorted grid voltages.

The mandatory dead time of the semiconductor switches distorts the output voltages, which creates a response to other waveforms [10]–[12]. High gain of the grid-voltage feedforward has been shown to magnify harmonics arising from the dead-time effect [13], which is relatively hard to model accurately [14]. Thus, the grid voltage feedforward has a dualistic impact on the power quality; high feedforward gain mitigates the power quality issues arising from distorted grid voltage, but at the same time magnifies harmonics caused by the internal dead-time effect of the inverter [9]. This paper shows that the feedforward gain that minimizes the output current harmonics depends on the time-varying grid conditions and can be found adaptively.

While the literature has reported on adaptive control of the grid-voltage feedforward [8], [15], it has only done so from an impedance-based stability perspective. In the present paper, the grid-voltage feedforward gains are adaptively adjusted to minimize the total harmonic distortion (THD) of the inverter output current. The implementation includes the use of a perturb-and-observe (P&O) algorithm, which perturbs the feedforward gain and observes response from the output current THD. The P&O algorithm is most commonly the maximum-power-point tracking (MPPT) algorithm in the DC side of PV-systems [16]–[18], but it is applied here for the first time in the AC side. The simulation results show that the adaptive grid-voltage feedforward is an effective and simple method for improving the power quality over conventional implementations, especially in varying grid conditions.

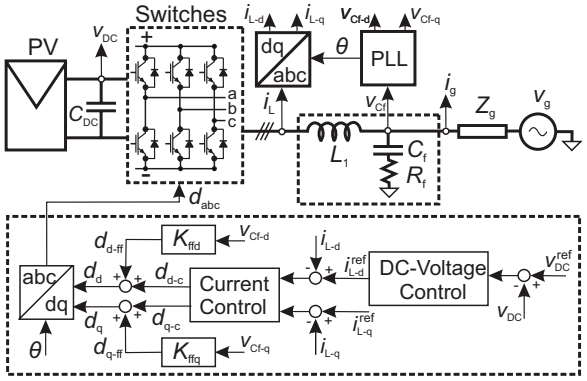

Fig. 1: Dq-domain control of grid-connected inverter.

The remainder of this paper is organized as follows. Section II provides some background to the grid-connected converter control strategy and the impact of its dead time. Section III introduces the use of the P&O algorithm in the converter AC side to adaptively adjust the feedforward gain to minimize the THD of the output current. Section IV shows the simulation results of the applied adaptive feedforward, which is capable of adjusting gains so that the output current THD is also minimized in rapidly changing grid conditions. Section V concludes.

II. Theory

A. Control of Grid-Connected Inverter

Three-phase AC systems can be analyzed in the synchronous-reference frame (dq domain) where the AC waveforms are transferred to two DC-valued signals by applying Park's transformation. The signals are referred to as direct (d) and quadrature (q), and the transformation also introduces crosscouplings between the two channels. The DC-valued signals allow linearization around the steady-state operating point, and thus the derivation of small-signal model with which the controllers can be designed [19].

Fig. 1 shows a three-phase grid-connected inverter with a cascaded control system, where d and q channels have separate control schemes. Inverter open-loop small-signal transfer functions can be represented as [20]

$$\begin{bmatrix} \hat{\mathbf{v}}_{\text{DC}} \\ \hat{\mathbf{i}}_{\text{L}} \end{bmatrix} = \begin{bmatrix} \mathbf{Z}_{\text{in-o}} & \mathbf{T}_{\text{oi-o}} & \mathbf{G}_{\text{ci-o}} \\ \mathbf{G}_{\text{io-o}} & -\mathbf{Y}_{\text{o-o}} & \mathbf{G}_{\text{co-o}} \end{bmatrix} \begin{bmatrix} \hat{\mathbf{i}}_{\text{DC}} \\ \hat{\mathbf{v}}_{\text{Cf}} \\ \hat{\mathbf{d}} \end{bmatrix} \tag{1}$$

The control is synchronized to grid voltages using a phase-locked loop (PLL) that provides synchronization angle (θ) for the dq-domain control. The outer control loop is a DC-voltage control, which provides the reference for d channel of the inner AC-current control loop, while its q channel regulates reactive current to zero for unity power factor. The grid-voltage feedforward is an additional control scheme that is used to improve the power quality.

The harmonics in the grid voltages circulate to inverter output currents through the inverter output admittance $Y_{\text{o-o}}$,

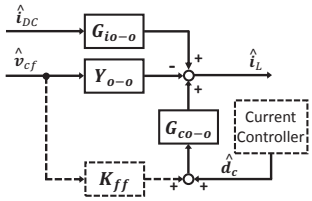

Fig. 2: Output dynamics of the grid-connected inverter.

thereby decreasing the power quality. The grid-voltage feedforward is used to mitigate the effect of low-order harmonics by adding the sensed grid voltages ($\hat{\mathbf{v}}_{\text{Cf-d}}$ and $\hat{\mathbf{v}}_{\text{Cf-q}}$) through an appropriate feedforward gain ($\mathbf{K}_{\text{ff}}$) to the duty ratios ($\mathbf{d}$). Fig. 2 shows the output dynamics of the inverter, from which the inverter output current can be derived as

$$\hat{\mathbf{i}}_{\text{L}} = \mathbf{G}_{\text{io-o}}\hat{\mathbf{i}}_{\text{DC}} - (\mathbf{Y}_{\text{o-o}} - \mathbf{G}_{\text{co-o}}\mathbf{K}_{\text{ff}})\hat{\mathbf{v}}_{\text{cf}} + \mathbf{G}_{\text{co-o}}\hat{\mathbf{d}}_{\text{c}} \tag{2}$$

The applied open-loop transfer functions are introduced in (1) and $\mathbf{K}_{\text{ff}}$ is a feedforward gain matrix. To fully compensate the $\mathbf{Y}_{\text{o-o}}\hat{\mathbf{v}}_{\text{cf}}$, the feedforward gain should be adjusted as $\mathbf{K}_{\text{ff}} = \mathbf{G}_{\text{co-o}}^{-1}\mathbf{Y}_{\text{o-o}}$. The equation may yield high-order transfer functions for $\mathbf{K}_{\text{ff}}$, which depends on the applied grid-side filter. However, high-order transfer functions as feedforward gains are sensitive for disturbances due to derivative terms. Fortunately, the equation is satisfied relatively accurate for L-filtered inverter (current feedback from inductor current, as shown in Fig. 1) by only the static gains ($1/V_{\text{DC}}$) in direct channels. Thus, the commonly applied transfer matrix for the grid-voltage feedforward is given as [9]

$$\mathbf{K}_{\text{ff}} = \begin{bmatrix} 1/V_{\text{DC}} & 0 \\ 0 & 1/V_{\text{DC}} \end{bmatrix} \tag{3}$$

In the ideal case, these gains remove the impact of the grid voltages from the produced output current, thus improving the power quality and decreasing the total harmonic distortion (THD) under distorted grid voltages.

B. Dead-Time

Three-phase inverters typically include six semiconductor switches, positive- and negative-leg switches for every phase. If both switches of the same phase are in the conductive mode, the DC link is short-circuited. The fact that real switches cannot change their state instantaneously must be taken into account to avoid short-circuiting the DC capacitor. Therefore, the dead time must be added into control system, which can be implemented by delaying the switch's turn-on signals by a certain amount of time to guarantee that the other switch always has time to change the mode to a non-conductive state. The dead time is usually a few percent of the inverter's switching cycle [13].

Apart from being important for avoiding short circuits, the dead time introduces momentary loss of controllability and reduces power quality [10]. Anti-parallel diodes are added to switching components to provide route for power flow during dead time. The conduction of the diodes causes distortion to the output voltages - mainly the 5th, 7th, 11th and 13th

harmonics - and their response to the output currents [11], [12]. The phenomena are relatively hard to model accurately because of non-linear characteristics and the complex dependency of many parameters [14].

It has been shown in [13] that the grid-voltage feedforward increases the harmonics caused by the dead-time effect when grid impedance is present. Because of the non-linear effect of the dead-time, it was not included in the linearized small-signal model of the inverter, from which the ideal gains for the feedforward were derived. Thus, the feedforward gain that minimizes the produced THD can be significantly lower than $1/V_{\text{DC}}$ as higher gains magnify the dead-time effect.

III. Methods

A. Perturb and Observe

The P&O algorithm is widely used in PV systems' maximum power-point tracking (MPPT) for optimizing the energy yield. The popularity of the algorithm is based on its simple implementation, where the PV-array voltage is perturbed and the output power is observed. If the output power increases, the next step is taken in the same direction; if the power is decreased, the next step is taken in the opposite direction. [17]

The P&O algorithm effectively finds the maximum or minimum value, at least the local one, of the observed variable in function of the perturbed one. However, a drawback of the algorithm is that it continues perturbations even when the maximum (minimum) value has been found. Thus, the algorithm makes the perturbed variable oscillate around the desired value. The oscillation amplitude is equal to the applied perturbation-step size (A_{pert}). [16] A lower step size indicates slow tracking in changing conditions, whereas higher steps increase oscillations. The step size should be high enough to perturb the system so that the increase or decrease in the observed value can be detected. Another critical value of the P&O algorithm is the time interval between the perturbations (T_{pert}), which should be longer than the system settling time, caused by the perturbation, to avoid misleading observations [18]. However, longer time intervals make the P&O algorithm slower in terms of finding the desired values after a change in operation conditions or during start-up. In changing conditions, a large step size with short time intervals between the perturbations is most desirable for fast performance. In steady conditions, an overly large step size and overly frequent perturbations increase oscillations around the desired values.

B. Adaptive Grid-voltage Feedforward to Minimize THD

The grid-voltage feedforward gains have a dualistic impact on the produced THD: higher gains mitigate the impact of the grid voltage harmonics and magnify the effect of the dead time. [9] Thus, highly distorted grid voltages endorse the use of high feedforward gains, while the ideal grid voltages endorse the gains near zero. A single inverter usually does not have information about the time-variant grid conditions. Additionally, the non-linear effect of the switches' dead time is not included in inverter models to accurately predict its impact on the produced THD, at least not yet. The ideal feedforward gain from the dead-time perspective equals to zero while it equals $1/V_{\text{DC}}$ to remove the impact of the grid-voltage harmonics. Thus, the feedforward gain that minimizes the produced THD depends on the operating conditions lies between zero and $1/V_{\text{DC}}$, and can be adaptively found by applying the P&O algorithm.

Due to time-varying and unpredictable operating conditions of the grid-connected inverter, the P&O algorithm is applied to adaptively adjust the grid-voltage feedforward gains to minimize the output current THD. Fig. 3 shows a block diagram of the adaptive-control scheme and the applied P&O algorithm in it. The grid-voltage feedforward gains are perturbed and the THD of the phase-domain output currents is observed. The direction of the next perturbation step in the feedforward gains is based on the observed THD. If the THD decreases because of the last taken step in feedforward gains, the next step is taken in the same direction. If the THD is increased, the direction of the perturbation steps is changed.

The feedforward gains are adaptively adjusted for d and q channels symmetrically. The perturbation size for adaptive feedforward gain is chosen as $A_{\text{pert}} = 0.05/V_{\text{DC}}$, the impact of which can be seen from the output current THD, but does not produce overly high oscillations when the THD-minimizing feedforward gains are found. Based on the approximated settling time of the system, the interval between perturbations is chosen as $T_{\text{pert}} = 0.2$ s, which determines the triggers executing the P&O algorithm. To avoid misleading disturbances, the THD is averaged over 0.15 s. It is observed after 0.2 s from the last perturbation and the direction of the next step is chosen.

IV. Experiments

The introduced approach for the grid-voltage feedforward is tested with a switching model of the three-phase grid-connected inverter in MATLAB/Simulink and compared to the conventional feedforward implementations. In all simulations, constant 2.7 kW DC power is fed to the (60 Hz/120 V) grid through the inverter and LC filter (C_{f}= 10 μF, L_{f} = 2.2 mH). The inverter dead time is included in the model by delaying the turn-on signals of the switches where the switching frequency equals 8 kHz. The grid impedance is passive (R_{g} = 0.4 Ω, L_{g} = 0.9 mH) and the grid-voltage disturbances are realized by introducing harmonics to grid-voltage reference, generated by an ideal voltage source. The DC voltage that affects the feedforward gains is kept at the maximum power point (414 V) in all simulations.

A. Dead-Time Effect

The required dead time of the semiconductor switches is usually a few percent of the switching cycle. Longer (safer) dead times distort the output voltages more, which increases the output current THD, especially when high gains in the grid-voltage feedforward are applied. Fig. 4 shows the output current THD when the feedforward gain is scanned from 0 to $1.1/V_{\text{DC}}$. Simulations in similar grid conditions (high harmoncis in grid voltages) with five inverters, in which only the dead time varies from 1 to 5 μs, equal 0.8-4 percent

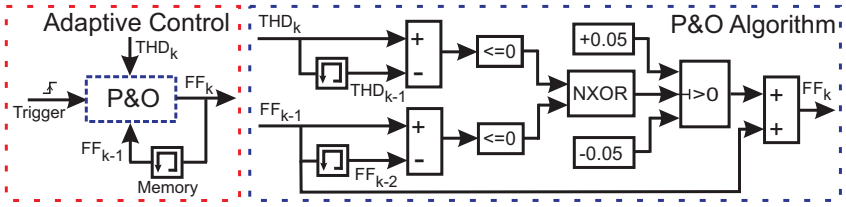

Fig. 3: Block diagram of the adaptive-control implementation.

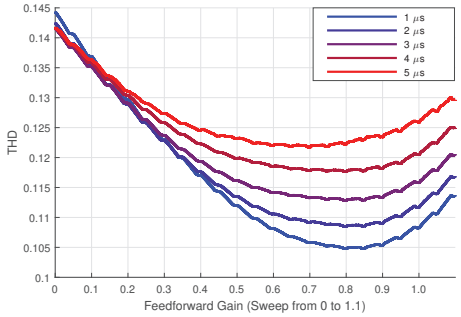

Fig. 4: Sweep of feedforward gain with different inverter dead times.

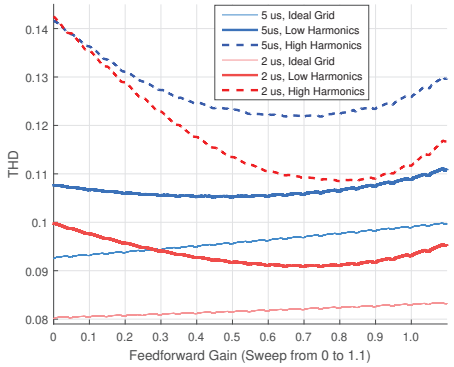

Fig. 5: Scan of feedforward gains with different dead times and grids.

of the applied switching cycle. Two important conclusions can be made from Fig. 4. First, the feedforward gains that minimize the output current THD can be found and they are not the conventionally adjusted 0 or $1/V_{\text{DC}}$; secondly, the THD increases with longer dead times when high feedforward gains are applied. The THD-minimizing gain is approximately $0.7/V_{\text{DC}}$ with 5 μs dead time and $0.85/V_{\text{DC}}$ with 1 μs. For example, with 1 μs dead time, the $0.85/V_{\text{DC}}$ feedforward gain produces approximately 26 percent lower output current THD than zero gain, and 3 percent lower than $1/V_{\text{DC}}$.

B. Grid Harmonics

As the grid-voltage feedforward has a dualistic impact on the power quality, the interfaced grid conditions and the dead time affect its performance. Fig. 5 shows the output current THD in three different grid conditions when the feedforward gains are varied from 0 to $1.1/V_{\text{DC}}$. Similar tests are made with two inverters applying 2 μs (red lines) and 5 μs (blue lines) dead times, equaling 1.6 and 4 percent of the switching cycle, respectively. The conditions are varied by changing the amount of harmonics in the grid voltages: ideal 60 Hz sinusoid (thin lines), low harmonic content (thick lines), and high harmonic content (dashed lines). Table I shows the THD-minimizing gains for every six cases. Under ideal 60 Hz grid voltages, the feedforward magnifies harmonics arising from the dead-time effect, and thus the THD-minimizing gain equals to zero. Under distorted grid voltages, the THD-minimizing gain is located between 0 and $1/V_{\text{DC}}$, which depends on both dead time and the amount of harmonics in grid voltages.

TABLE I: THD-minimizing gains

		Grid harmonics		
		Ideal	Low	High
Dead time	2 μs	0.00	$0.70/V_{\text{DC}}$	$0.85/V_{\text{DC}}$
	5 μs	0.00	$0.50/V_{\text{DC}}$	$0.70/V_{\text{DC}}$

Fig. 5 shows that longer dead time supports the use of lower feedforward gains, while increased grid-voltage harmonics endorse higher gains. The THD-minimizing gain under highly distorted grid voltages and 2 μs dead time is $0.85/V_{\text{DC}}$, with which the output current THD is decreased by approximately 23 percent compared to zero gain and 4 percent compared to $1/V_{\text{DC}}$. In this case, the THD-minimizing gain is high because of the relatively short dead time and highly distorted grid voltages. Under low grid harmonics and 5 μs dead time, the THD-minimizing gain ($0.50/V_{\text{DC}}$) is lower and the THD can be decreased 1 percent compared to zero gain and 2 percent compared to $1/V_{\text{DC}}$.

C. Perturb and Observe during Start-up

The P&O algorithm adaptively adjusts the feedforward gains to minimize the output current THD. The implementation has a plug-and-play feature during start-ups as the algorithm independently finds the gains that minimize the output current THD in interfaced grid conditions. Fig. 6 shows the THD of the output current and the feedforward gain during the inverter start up in two different grid conditions, with low (left) and high (right) harmonic content in the grid voltages. The inverter dead time is 5 μs in both cases. After an experimentally approximated settling time of the start-up (0.5 s), the P&O algorithm is enabled at 0.6 s. The feedforward gain increases by $A_{\text{pert}} = 0.05/V_{\text{DC}}$ in $T_{\text{pert}} = 0.2$ s intervals until the THD-minimizing gain is achieved. Those gains are $0.5/V_{\text{DC}}$ and $0.7/V_{\text{DC}}$ for grids with low and high harmonics, respectively. The THD is decreased by 3 percent when the inverter is interfacing to low-harmonic grid voltages, and 14 percent when there are high harmonics.

The drawback of the P&O algorithm is that the gains start oscillating around the THD-minimizing gain by A_{pert}. The

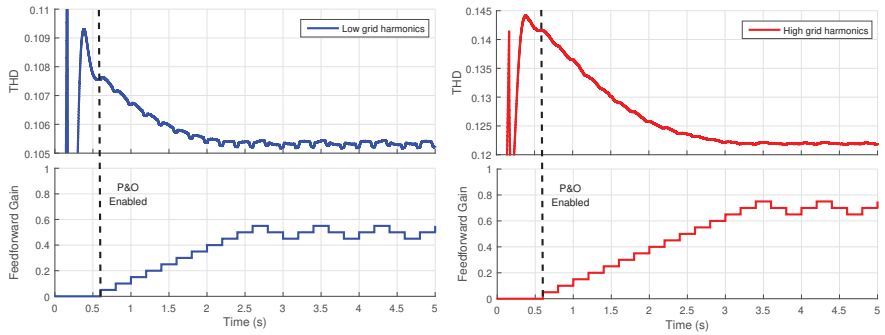

Fig. 6: Perturb and observe performance during start-ups in different grids.

feedforward gain remains at the THD-minimizing gain half of the oscillation cycle (4 T_{pert}), while the gain is improperly adjusted by A_{pert} during the other half of the cycle. However, the effect to the THD is negligible compared to the benefits of the adaptive grid-voltage feedforward compared to the conventional implementation with zero or $1/V_{\text{DC}}$ gains.

D. THD Minimization during Transient Cases

The grid conditions may significantly vary over time, especially the distortions in voltages when local production and loading profiles change [5], [6]. Fig. 7 shows the performance comparison between the conventional (constant zero and $1/V_{\text{DC}}$ gains) and the adaptive feedforward implementations under varying grid conditions. First, the inverter with 5 μs dead time is started up under ideal 60 Hz grid voltages, at 2 s and 10 s the harmonics in grid voltages are suddenly increased. Before 2 s, the adaptively adjusted feedforward gain oscillates around zero. It may be obvious that the THD is similar with the conventional zero gain. The THD is 5 percent higher with $1/V_{\text{DC}}$. After the first increase in grid-voltage harmonics, both constant gains $1/V_{\text{DC}}$ and zero gain produces approximately same amount of THD. It takes 2.4 s for the P&O to find the THD-minimizing gain ($0.6/V_{\text{DC}}$) under slightly distorted grid voltages; with that gain, the produced THD is 8 percent lower compared to constant zero and $1/V_{\text{DC}}$ gains. After the second transient in grid conditions, it takes 1.6 s for adaptive implementation to find the new THD-minimizing gain ($0.9/V_{\text{DC}}$). The THD-minimizing gain produces 21 percent lower THD than constant zero gain, and over 7 percent lower than $1/V_{\text{DC}}$ gain. Thus, it can be concluded that the presented adaptive implementation also improves the performance of the grid-voltages feedforward in changing grid conditions.

Figs. 8 and 9 take a closer look at the effect of the feedforward gains by showing a magnitude of the output current harmonics under low and high grid harmonics, which are measured between 7 - 9 s and 12 - 14 s, respectively, in the same simulation as analyzed in Fig. 7. The amount of harmonics are shown in Table II; the highest amounts are emboldened to highlight the clear effect of the feedforward gain. Higher feedforward gains effectively mitigate the low-order harmonics that arise from the grid voltages, especially 3 rd and 5 th. For example, during high grid harmonics (Fig. 9), the 3 rd harmonic can be mitigated over by 70 percent by using

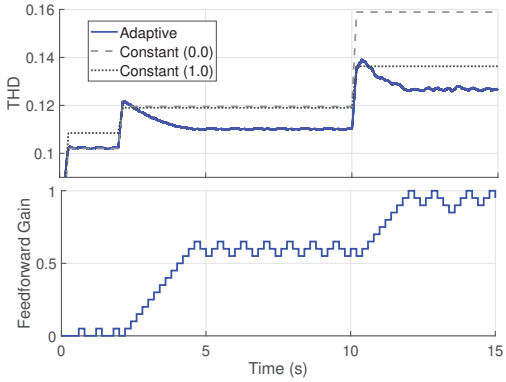

Fig. 7: Performance comparison during grid transients.

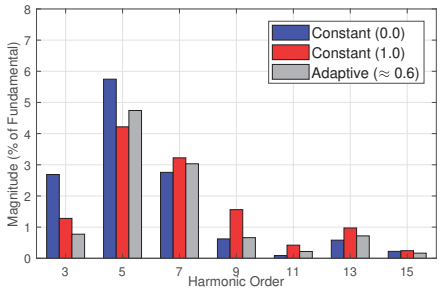

Fig. 8: Output current harmonics under slightly distorted grid.

$1/V_{\text{DC}}$ gain, and over 60 percent with adaptive ($\approx 0.9/V_{\text{DC}}$) gain when compared to the constant zero gain. However, high feedforward gain magnifies higher-order harmonics arising from the inverter dead-time effect. For example during low grid harmonics (Fig. 8), the 11 th harmonic increases by over 350 percent with $1/V_{\text{DC}}$ gain and by almost 150 percent with adaptive gain ($\approx 0.6/V_{\text{DC}}$) when compared to the constant zero gain. It should be noted that absolute values of the high-order harmonics remains significantly smaller than low-order harmonics. Thus, the percentage increment in the high-order harmonics has less impact in the output current THD than low-order harmonics.

The harmonics in grid voltages circulate to the inverter output currents. High feedforward gains effectively mitigate the impact of the grid-voltage harmonics by decreasing low-order harmonics in the output currents; at the same time, they magnify the dead-time effect, which appears as increased high-

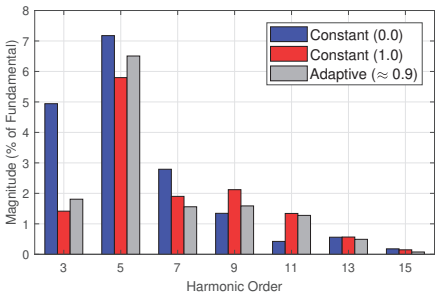

Fig. 9: Output current harmonics under highly distorted grid.

TABLE II: Amount of harmonics

	Grid harmonics					
	Low			High		
	0	1	≈ 0.60	0	1	≈ 0.90
3 rd	**2.688**	1.280	0.773	**4.942**	1.416	1.808
5 th	**5.747**	4.218	4.742	**7.176**	5.798	6.507
7 th	2.757	**3.223**	3.032	**2.791**	1.901	1.560
9 th	0.622	**1.560**	0.662	1.345	**2.121**	1.588
11 th	0.089	**0.421**	0.218	0.424	**1.341**	1.277
13 th	0.582	**0.973**	0.719	0.561	**0.567**	0.492
15 th	0.223	**0.244**	0.165	**0.179**	0.147	0.076

order harmonics. For every realistic case, there appears to be an optimal feedforward gain between zero and $1/V_{\text{DC}}$, which balances the dualistic impact of the grid-voltage feedforward by minimizing the output current THD. The value of the optimal gain is based on the amount of the grid-voltage harmonics and can be found adaptively, without prior knowledge about the grid conditions, by using the proposed P&O algorithm.

V. Conclusions

This paper has presented an adaptive grid-voltage feedforward for grid-connected inverters. In the method, the feedforward gains are adaptively adjusted so that the output current THD is minimized, thus improving the power quality. The grid-voltage feedforward is shown to have dualistic impact on the produced power quality; it mitigates disturbances from grid voltages, but also magnifies the harmonics arising from the inverter dead-time effect. Hence, the optimal gain in perspective of minimizing the output current THD depends on the interfaced grid conditions, which may vary over time. This makes the feedforward gains attractive choice for including adaptive operations. The presented adaptive-control method includes the use of the P&O algorithm for the first time in AC sides. The presented method perturbs the feedforward gains and observes the impact on the produced power quality (current THD). This novel approach includes a plug-and-play feature during start-up and fast adaptivity to changes in grid conditions. Through simulations, the adaptive grid-voltage feedforward is shown to improve the system performance and the produced power quality in various grid conditions compared to conventional implementations.

References

[1] B. K. Bose, "Global energy scenario and impact of power electronics in 21st century," *IEEE Transactions on Industrial Electronics*, vol. 60, no. 7, pp. 2638–2651, 2013.

[2] C. Li, "Unstable operation of photovoltaic inverter from field experiences," *IEEE Transactions on Power Delivery*, vol. 33, no. 2, pp. 1013–1015, 2018.

[3] L. Wang, X. Xie, Q. Jiang, H. Liu, Y. Li, and H. Liu, "Investigation of ssr in practical dfig-based wind farms connected to a series-compensated power system," *IEEE Transactions on Power Systems*, vol. 30, no. 5, pp. 2772–2779, Sep. 2015.

[4] J. M. Carrasco, L. G. Franquelo, J. T. Bialasiewicz, E. Galvan, R. C. PortilloGuisado, M. A. M. Prats, J. I. Leon, and N. Moreno-Alfonso, "Power-electronic systems for the grid integration of renewable energy sources: A survey," *IEEE Transactions on Industrial Electronics*, vol. 53, no. 4, pp. 1002–1016, June 2006.

[5] Q. Zhong and T. Hornik, "Cascaded current–voltage control to improve the power quality for a grid-connected inverter with a local load," *IEEE Transactions on Industrial Electronics*, vol. 60, no. 4, pp. 1344–1355, April 2013.

[6] Q. Trinh and H. Lee, "An enhanced grid current compensator for grid-connected distributed generation under nonlinear loads and grid voltage distortions," *IEEE Transactions on Industrial Electronics*, vol. 61, no. 12, pp. 6528–6537, Dec 2014.

[7] Q. Yan, X. Wu, X. Yuan, and Y. Geng, "An improved grid-voltage feedforward strategy for high-power three-phase grid-connected inverters based on the simplified repetitive predictor," *IEEE Transactions on Power Electronics*, vol. 31, no. 5, pp. 3880–3897, May 2016.

[8] M. Cespedes and J. Sun, "Adaptive control of grid-connected inverters based on online grid impedance measurements," *IEEE Trans. on Sustainable Energy*, vol. 5, pp. 516–523, 2014.

[9] T. Messo, R. Luhtala, A. Aapro, and T. Roinila, "Accurate impedance model of grid-connected inverter for small-signal stability asssessment in high-impedance grids," in *IEEJ Journal of Industry Applications*, vol. 8, 2019, pp. 488–492.

[10] S.-G. Jeong and M.-H. Park, "The analysis and compensation of dead-time effects in pwm inverters," *IEEE Transactions on Industrial Electronics*, vol. 38, no. 2, April 1991.

[11] Z. Shen and D. Jiang, "Dead-time effect compensation method based on current ripple prediction for voltage-source inverters," *IEEE Transactions on Power Electronics*, vol. 34, no. 1, pp. 971–983, Jan 2019.

[12] G. Grandi, J. Loncarski, and R. Seebacher, "Effects of current ripple on dead-time distortion in three-phase voltage source inverters," in *2012 IEEE International Energy Conference and Exhibition (ENERGYCON)*, Sep. 2012, pp. 207–212.

[13] T. Messo, T. Roinila, A. Aapro, and P. Rasilo, "Evaluation of dead-time effect of grid-connected inverters using broadband methods," in *18th IFAC Symposium on System Identification*, 2018.

[14] I. Dolguntseva, R. Krishna, D. E. Soman, and M. Leijon, "Contour-based dead-time harmonic analysis in a three-level neutral-point-clamped inverter," *IEEE Transactions on Industrial Electronics*, vol. 62, no. 1, pp. 203–210, Jan 2015.

[15] R. Luhtala, T. Messo, and T. Roinila, "Adaptive control of grid-voltage feedforward for grid-connected inverters based on real-time identification of grid impedance," in *IPEC-Niigata 2018 -ECCE ASIA*, 2018, pp. 1–8.

[16] N. Femia, G. Petrone, G. Spagnuolo, and M. Vitelli, "Optimization of perturb and observe maximum power point tracking method," *IEEE Transactions on Power Electronics*, vol. 20, no. 4, pp. 963–973, July 2005.

[17] D. Sera, L. Mathe, T. Kerekes, S. V. Spataru, and R. Teodorescu, "On the perturb-and-observe and incremental conductance mppt methods for pv systems," *IEEE Journal of Photovoltaics*, vol. 3, no. 3, pp. 1070–1078, July 2013.

[18] M. A. Elgendy, B. Zahawi, and D. J. Atkinson, "Operating characteristics of the p o algorithm at high perturbation frequencies for standalone pv systems," *IEEE Transactions on Energy Conversion*, vol. 30, no. 1, pp. 189–198, March 2015.

[19] T. Messo, A. Aapro, and T. Suntio, "Generalized multivariable small-signal model of three-phase grid-connected inverter in dq-domain," in *2015 IEEE 16th Workshop on Control and Modeling for Power Electronics (COMPEL)*, 2015.

[20] R. Luhtala, T. Reinikka, T. Roinila, T. Messo, and J. Sihvo, "Improved real-time stability assessment of grid-connected converters using mimo-identification methods," in *2018 IEEE Energy Conversion Congress and Exposition (ECCE)*, 2018.